


Statistics of Colloidal Suspensions Stirred by Microswimmers

Levke Ortlieb,¹ Salima Rafai,³ Philippe Peyla,³ Christian Wagner,^{1,2} and Thomas John^{1,*}

¹Universität des Saarlandes, Postfach 151150, D-66041 Saarbrücken, Germany

²University of Luxembourg, L-1511 Luxembourg, Luxembourg

³University Grenoble Alpes, CNRS, LIPhy, F-38000 Grenoble, France

 (Received 19 September 2018; revised manuscript received 11 March 2019; published 9 April 2019)

We present a statistical analysis of the experimental trajectories of colloids in a dilute suspension of the green algae *Chlamydomonas reinhardtii*. The measured probability density function (pdf) of the displacements of colloids covers 7 orders of magnitude. The pdfs are characterized by non-Gaussian tails for intermediate time intervals, but nevertheless they collapse when scaled with their standard deviation. This *diffusive scaling* breaks down for longer time intervals and the pdf becomes Gaussian. However, the mean squared displacements of tracer positions are linear over the complete measurement time interval. Experiments are performed for various tracer diameters, swimmer concentrations, and mean swimmer velocities. This allows a rigorous comparison with several theoretical models. We can exclude a description based on an effective temperature and other mean field approaches that describe the irregular motion as a sum of the fluctuating far field of many microswimmers. The data are best described by the microscopic model by J.-L. Thiffeault, Distribution of particle displacements due to swimming microorganisms, *Phys. Rev. E* **92**, 023023 (2015).

DOI: [10.1103/PhysRevLett.122.148101](https://doi.org/10.1103/PhysRevLett.122.148101)

Microscopic unicellular algae are abundant in the Earth's oceans, rivers, and lakes. They are crucial for the ecosystem because they contribute to an estimated 50% of the world's oxygen production [1,2]. In addition, it is suspected that they play an important role in stirring the top level of the oceans [3–6]. This so-called biogenetic mixing is important for the availability of nutrients for the survival of many organisms. In the presence of active microswimmers, a passive fluid is stirred and shows an *active* spatiotemporal random fluid motion. These fluctuations at the scale of microorganisms can be characterized by tracking suspended tracer particles such as microspheres [7]. They undergo both Brownian thermal motion and follow the active random fluid motion generated by swimmers. A seminal work was presented by Wu and Libchaber in 2000 [8], with a study on concentrated *Escherichia coli* bacteria suspensions. They report a non-Brownian, superdiffusive behavior of the mean squared displacement, $\text{MSD}(t)$, for short time intervals, but the colloids were much bigger than the bacteria. In 2009, Leptos *et al.* [9] presented experimental data on diffusing microspheres in a dilute suspension of the swimming algae *Chlamydomonas reinhardtii* (CR).

CR is a puller type swimmer and has become a standard for this type of microswimmers in many laboratory experiments [10]. Leptos *et al.* [9] observed a linear $\text{MSD}(t)$ with a *diffusive scaling* of the pdf of tracer displacements that could be rescaled with the standard deviation and remain self-similar despite being non-Gaussian. One class of models that can show such a behavior is known as continuous time random walk (CTRW)[11]. Other theoretical models predict that the scaling of the distribution

function is transient and disappears for longer measurements [12]. The experiments by Leptos *et al.* [9] were followed by several further experiments on biological microswimmers [13], artificial swimmers [14,15], and several theoretical models [11,12,16–20]. We followed the experimental concept of Leptos *et al.* [9] but with the following extension: we used colloids ranging from sizes smaller to larger (compared to the swimmers) and two algae strains with significantly different speeds. Our essentially improved statistics allowed us to obtain the details of the pdf at the low-probability tails and long trajectories to demonstrate the breakdown of the non-Gaussian behavior of the pdf. This allowed us to exclude several theoretical and phenomenological explanations and descriptions. Furthermore, we could conclusively answer a key question: until which time scales can the enhanced diffusivity be described by the short-time interactions between single swimmers and tracers? Therefore, we analyze (1) the MSD of trajectories of tracer particles with various diameters for two different swimmer velocities, (2) the non-Gaussian shape of the pdf($x; t$) at a fixed time difference, and (3) the temporal propagation of the pdf and its kurtosis in order to quantify for the non-Gaussianity and the breakdown of diffusive scaling as proposed in Ref. [12].

Experiments were performed with an Eclipse TE-2000-S Nikon microscope with a 4× objective (NA = 0.2) and a Flea3 FL3-U3-88S2C-CMOS-camera at a frame rate of 60 Hz and with a resolution of 2048 × 1080 px. This relatively small magnification results in a very large field of view (1.56 × 0.82 mm) and the depth of field (more than 50 μm), so that we can follow the 2D projection of the 3D

motion of hundreds of colloids in focus for several minutes, which is favorable for good statistics compared to a more precise determination of the position with a higher magnification [21]. The suspensions were observed in microscopy chambers (ibidi®, μ -Slide VI 0.4) with a thickness of $400\ \mu\text{m}$ in the direction of gravity and a lateral extension of $3.8 \times 17\ \text{mm}$. The middle of the chamber was in focus to exclude boundary effects. The specific swimmer number density was determined immediately before performing an experiment by counting the swimmers in self-made chambers of $60\ \mu\text{m}$ height. At our low-number densities, miscounts due to overlaps could be excluded but due to sample inhomogeneities and local density variations, the maximal error in swimmer number densities is estimated to be 25%. Image sequences were recorded by dark-field microscopy. A red light source ($\lambda > 600\ \text{nm}$) was used for illumination at low intensities because the strains of CR (WT.T222-mt+ and SAG 11-32c-mt) are phototactic for shorter wavelengths. We took special care to obtain almost identical diameters of the CR of approximately $10\ \mu\text{m}$ by ensuring that cells were in the same stage of their life cycle. The algae were grown in TAP medium at temperature $T = (296 \pm 1)\ \text{K}$, and the viscosity of the suspending medium was $\eta = (0.95 \pm 0.1)\ \text{mPa}\cdot\text{s}$ [22]. The mean velocities of the strains WT.T222 mt+ and SAG 11-32c-mt- are $U = (35 \pm 10)\ \mu\text{m}/\text{s}$ and $(70 \pm 20)\ \mu\text{m}/\text{s}$, respectively. The latter has a faster flagella frequency and is referred to as “fast swimmer” hereafter. We use mono-disperse ($\sigma < 5\%$) uncoated polystyrene microspheres as colloids (Fluka/Sigma Aldrich) with diameters d between 1 and $20\ \mu\text{m}$. They have a density of $1.05\ \text{g}/\text{cm}^3$ and for experiments with particles larger than $3\ \mu\text{m}$ a density matching with a suitable mixture of water and heavy water (D_2O) was necessary to avoid sedimentation. In these experiments, the algae were grown in TAP medium and heavy water was added shortly before the experiment. The swimming speed of the algae in the solution with D_2O did not

change compared to the standard solution within an hour, but the algae did not survive for more than a few hours. The slight viscosity increase due to the heavy water $\eta_{\text{D}_2\text{O}+\text{H}_2\text{O}}/\eta_{\text{H}_2\text{O}} > 1$ is taken into account as a correction for the effective diffusion coefficient, for the purpose of direct comparison with experiments in the standard solution. The diffusion coefficient for Brownian motion is given by the Stokes-Einstein relation $D_0 = k_B T / (6\pi\eta R)$ with tracer radius R and temperature T . To extract the trajectories from image sequences, we used a MATLAB®-based software developed by our group [21,23]. The sup-pixel resolution of $0.1\ \mu\text{m}$ of tracer positions is achieved by intensity weighted centroid determination.

Figures 1(a) and 1(c) show the trajectories of two tracer particles of different sizes at a moment when a swimmer passes close by. Thermal noise results in a typical Brownian motion and the concomitant random displacements are proportional to the size of the particles. During the short time interval when the swimmer is close to the tracer, the latter performs a large, looped motion, shown in Fig. 1(a). According to Refs. [12,24], those loops mainly contribute to the observed enhanced diffusivity. Note that in our setup, we did not observe that a tracer was carried by a swimmer over unexpectedly long distances [13]. The observed duration of the interaction of a tracer with a swimmer is very small compared to the full trajectory. This is visualized by the color code in Fig. 1(a). Figure 1(b) shows a simulation of a tracer trajectory with a passing swimmer modeled as a squirmer, including the contribution of thermal Brownian noise. A squirmer is a model for an active moving sphere in Stokes flow. The so-called squirmer parameter β defines whether the flow field is comparable to a pusher or puller [25]. We reproduced the simulations described in Ref. [12]. In contrast to Brownian motion, the size of the loops due to passing swimmers is independent of the size of the tracer, shown in Fig. 1(c).

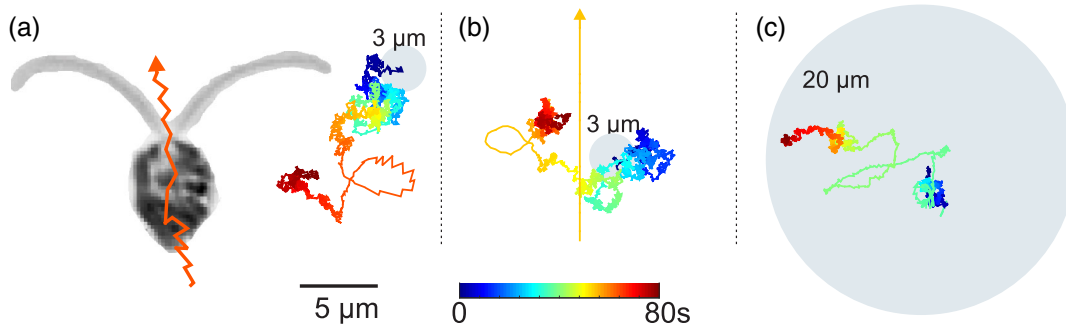


FIG. 1. Microscope image of a microswimmer, sketches of colloids, and tracer trajectories. Color encodes the time. The sketched microspheres (gray disks) and the swimmer are scaled. (a) Trajectory of a microsphere over 80s and a short part of the swimmer trajectory at around $t \approx 70\ \text{s}$. At the moment of interaction, the irregular Brownian motion of the tracer is superimposed on a loop. (b) Simulated trajectory with a similar loop due to a spherical squirmer with a speed of $U = 35\ \mu\text{m}/\text{s}$ and a radius $\ell = 6\ \mu\text{m}$ moving along the direction of the arrow at $t \approx 60\ \text{s}$ [12]. A representative thermal Brownian motion was added. (c) Experimental trajectory of a much bigger sphere interacting with a swimmer (not shown) at $t \approx 40\ \text{s}$. In this case, the Brownian motion is less pronounced, but the size of the loop is comparable to (a),(b).

Figure 2(a) shows the MSDs. They were extracted by taking the time average for each trajectory followed by an ensemble average [21,26]. We found a perfect linear dependency $\text{MSD} \propto t$ over almost 3 orders of magnitudes for all particle diameters, swimmer number densities, and swimmer velocities. Only at short intervals, $t < 0.1$ s, the MSD deviates slightly from the linear slope due to uncorrelated position detection noise [26,27]. Based on this linearity, an effective diffusion coefficient can be defined as $\text{MSD}(t) = 4D_{\text{eff}}t$ for two spatial dimensions. Symbols in Fig. 2(b) show the effective diffusion coefficients, D_{eff} , as the function of the measured swimmer number density n . The lines represent the predictions for a squirmer model [12] [Eq. (27)]

$$D_{\text{eff}} = D_0 + \left(0.266 + \frac{3}{4}\pi\beta\right)Un\ell^4, \quad (1)$$

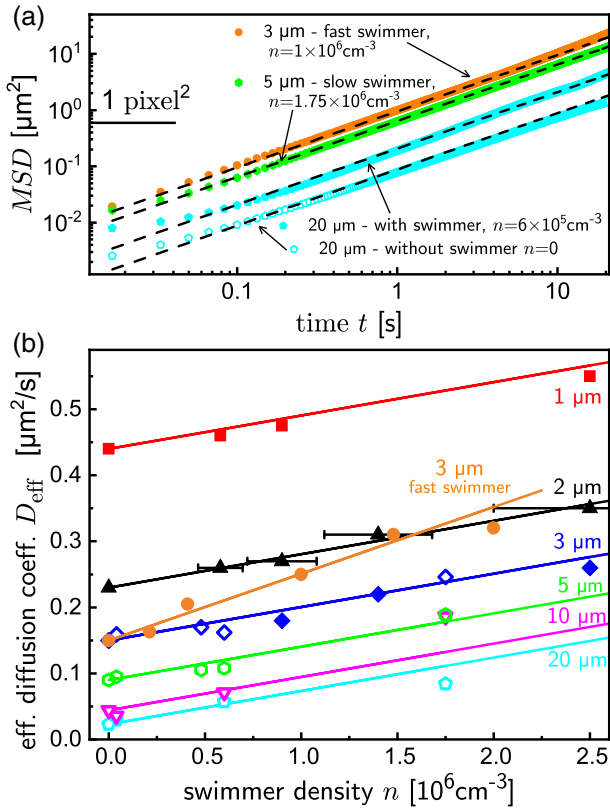


FIG. 2. (a) Mean squared displacements, MSDs, for various tracer diameters in the suspensions of slow and fast swimmers and without swimmers. (b) Effective diffusion coefficients vs swimmer number density n for various tracer diameters d of slow swimmers, and one example for fast swimmers. For particles with a diameter $d \geq 3 \mu\text{m}$, D_2O was added to the TAP solution to prevent sedimentation (open symbols). The lines correspond to predictions by Eq. (1). Error bars in swimmer densities are only shown for the $2 \mu\text{m}$ colloids. Errors bars in D_{eff} are of the order of the symbol size.

where U is the mean swimmer velocity, $\ell = 6 \mu\text{m}$ the radius of the squirmer, and $\beta = 0.6$ the fitted squirmer parameter. A positive $\beta > 0$ refers to a puller swimmer. The error bars in D_{eff} are smaller than the symbol size, and the Einstein-Stokes diffusion coefficients D_0 in pure TAP medium agree with the measured value in the range of few percent. The measured enhanced diffusion $D_{\text{eff}} - D_0$ is independent of the tracer size. As predicted by Eq. (1), the slope of swimmer density versus the effective diffusion of the fast strain with a double mean velocity is twice that of the slower swimmers. Therefore, we can exclude those characterizations where D_{eff} is associated with an effective temperature $k_{\text{B}}T_{\text{eff}} = 6\pi\eta R D_{\text{eff}}(n)$, because we found that the increment in the diffusivity is independent of the tracer diameter [8,28–31]. An effective temperature definition also requires a Maxwell-Boltzmann distribution in the velocities of the tracers, but this can be excluded because we observed a non-Gaussian probability density function for the displacements.

The probability density function $\text{pdf}(x;t)$ of tracer displacements contains more information than the MSD, the second moment $\text{MSD}(t) = \int x^2 \text{pdf}(x;t) dx$ of the distribution. Figure 3 shows an exemplary pdf from an experimental data set of length 300s with approximately 5×10^4 (partially fragmented) trajectories with a total of 3×10^7 data points. A local adaptive kernel density estimator was used to estimate the empirical pdf [32]. Only the right part of the pdf is shown because it is symmetric. The displacement is nondimensionalized $\hat{x} = x/(2D_{\text{eff}}t)^{1/2}$ according to the diffusive scaling introduced in Ref. [9]. At this low number density of $n = 1.5 \times 10^6 \text{ cm}^{-3}$, the mean interswimmer distance is $90 \mu\text{m}$ and we can exclude any collective behavior. The presented dataset strongly extends the data range presented in Ref. [9]. This allows us to compare our data with predictions from various models, in particular with respect to the non-Gaussian tails on a logarithmic scale over seven decades. The central part of the pdf is always Gaussian, due to the thermal motion of the colloids. The inset in Fig. 3 shows the power law tail $\text{pdf} \propto \hat{x}^{-4}$ predicted by Pushkin and Yeomans for dipolar swimmers such as CR [24] [Eq. (12)]. This behavior is also predicted by the microscopic model by Thiffeault [12], up to the distance where a cell swims within the time interval t . The authors in Ref. [9] fit their data with a superposition of a Gaussian and an exponential [33]. Our extended dataset is not well characterized by this functional approximation. Eckhard *et al.* [11] suggested a description in terms of a CTRW. One remarkable feature of a CTRW is that it is possible to construct random walks with a linear MSD in time but with an underlying non-Gaussian pdf. The CTRW presented in Ref. [11] predicts a self-similarity of the pdf with the appropriate scaling of space and time [34]. Such a self-similarity was already observed by Leptos *et al.* [9] and referred to as diffusive scaling. We fit our data to Eq. (3) in

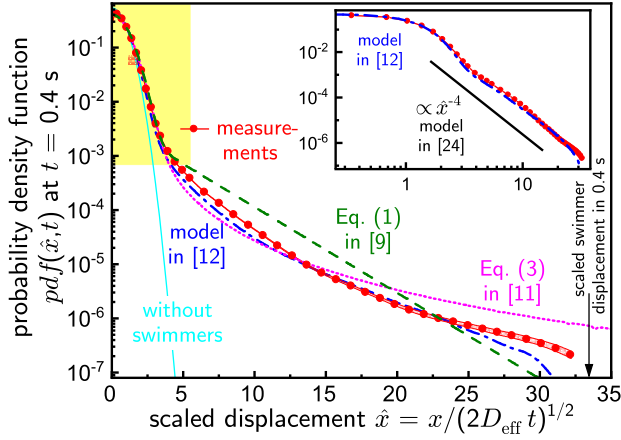


FIG. 3. Experimental pdf ($\hat{x}; t$) ($\bullet\text{---}\bullet$) at $t = 0.4$ s and a number density of $n = 1.5 \times 10^6 \text{ cm}^{-3}$ for colloids of $d = 3 \mu\text{m}$. The small red shadowed region indicates the 95% bootstrap confidence interval [36]. Various characterizations and predictions are shown: (---) a superposition of Gaussian and exponential, ($\text{---}\bullet\text{---}$) CTRW model, ($\text{---}\bullet\text{---}$) the microscopic model, and the asymptotic pdf $\propto \hat{x}^{-4}$ in the inset; see text for parameters. The measured pdf for pure Brownian motion is shown as (---). The yellow area indicates the data range presented in Ref. [9]. The black arrow indicates the scaled swimming distance of the microswimmers within 0.4 s.

Ref. [11]. Although the empirical MSD and pdf can be reproduced by the CTRW model, simulated trajectories never show loops as observed in experiment, as shown in Fig. 1. We also compare the experimental data with the microscopic model [12]. The calculated pdf deviates slightly from our empirical pdf, in particular at the far end of the tail. One reason for this is that the model squirmers with a single velocity U cover a maximum distance of $U \times t = 14 \mu\text{m}$ in the considered time interval of 0.4 s. This leads to a maximum tracer displacement caused by a single particle-swimmer interaction. In the experiments, the velocities follow a broad distribution and consequently the sharp drop in the pdf is softened [35].

During longer time intervals, several swimmer-tracer interactions occur, which result in additional, statistically independent displacements, and according to the central limit theorem the sum of many displacements yields a Gaussian pdf. This means that for longer time durations the enhanced diffusing coefficient D_{eff} should persist, but the non-Gaussianity and the associated diffusive scaling should break down. This is shown experimentally in Fig. 4 at $t \gtrsim 2$ s, where the pdf evolves toward a Gaussian. In contrast, the CTRW approach includes an intrinsic self-similarity for all times. In accordance with our measurements, the model by Thiffeault predicts the breakdown of the diffusive scaling, i.e., a transition from a non-Gaussian to a Gaussian pdf for longer time durations. Therefore, the pdfs cannot be scaled to collapse onto a single curve. However, the MSD is still linear throughout our

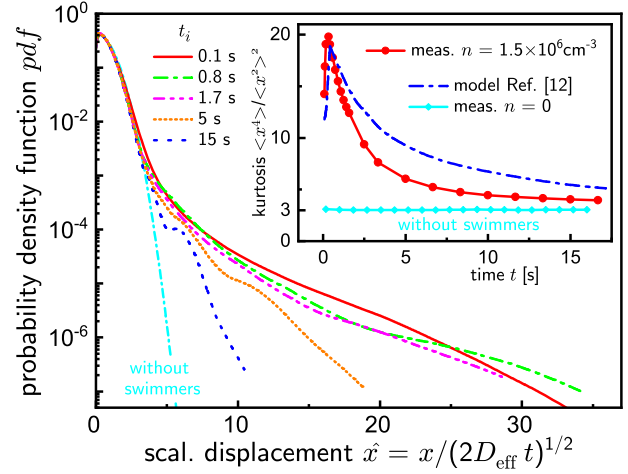


FIG. 4. Experimental pdf at $n = 1.5 \times 10^6 \text{ cm}^{-3}$ for various time intervals t_i to visualize the breakdown of the diffusive scaling. The pdf becomes a Gaussian for $t_i > 2$ s as predicted in Ref. [12]. The inset shows the kurtosis as measured to quantify the non-Gaussian tails.

measurements (see. Sec. VI in Ref. [12]). Another good measure to quantify the deviation from a Gaussian is the kurtosis κ , the fourth standardized moment, shown in the inset of Fig. 4. Both empirical kurtosis and the calculated kurtosis from the microscopic model agree reasonably well. The kurtosis is very sensitive to the tails of a distribution and a broad swimmer speed distribution might explain the remaining discrepancy (see also Supplemental Material [35]). The peak in the kurtosis, for ≈ 0.2 s, indicates the interaction time of a tracer with a swimmer. As expected, experiments without swimmers have a time independent $\kappa = 3$. The empirical approach in Ref. [9] for the pdf as a sum of a Gaussian and an exponential is time invariant and predicts a fixed $\kappa = 3.55$. The pdf of a CTRW decays as a power law [37] with an exponent lower than 4, so that the integral for the kurtosis does not converge. The same holds for the asymptotic prediction pdf $\propto \hat{x}^{-4}$ in [24] [Eq. (12)].

In conclusion, we have shown that the enhanced diffusion of tracer particles stirred by microswimmers is caused by rare events of single swimmer-tracer encounters, leading to looped tracer movements. The empirical pdf of tracer displacements allowed us to exclude several theoretical models. For intermediate time intervals, the pdf can be scaled to collapse onto a master curve referred to as diffusive scaling, but the scaling breaks down for longer times. We found that the microscopic model by Thiffeault [12] describes our data best for all time scales.

We gratefully acknowledge C. Ruloff, A. Morozov, and S. Zammert for their stimulating discussions. We acknowledge funding by the German French University (DFH-DFDK 01-14 Living Fluids). S.R. and P.P. thank the Labex Tec21 and ANR Jeunes Chercheuses, Jeunes Chercheurs for fundings.

- *thomas.john@physik.uni-saarland.de
- [1] C. B. Field, M. J. Behrenfeld, J. T. Randerson, and P. Falkowski, Primary production of the biosphere: Integrating terrestrial and oceanic components, *Science* **281**, 237 (1998).
- [2] J. S. Guasto, R. Rusconi, and R. Stocker, Fluid mechanics of planktonic microorganisms, *Annu. Rev. Fluid Mech.* **44**, 373 (2012).
- [3] M. M. Wilhelmus and J. O. Dabiri, Observations of large-scale fluid transport by laser-guided plankton aggregations, *Phys. Fluids* **26**, 101302 (2014).
- [4] E. Kunze, J. F. Dower, I. Beveridge, R. Dewey, and K. P. Bartlett, Observations of biologically generated turbulence in a coastal inlet, *Science* **313**, 1768 (2006).
- [5] A. W. Visser, Biomixing of the oceans?, *Science* **316**, 838 (2007).
- [6] A. M. Leshansky and L. M. Pismen, Do small swimmers mix the ocean?, *Phys. Rev. E* **82**, 025301(R) (2010).
- [7] E. M. Furst, *Microrheology* (Oxford University Press, New York, 2017).
- [8] X.-L. Wu and A. Libchaber, Particle Diffusion in a Quasi-Two-Dimensional Bacterial Bath, *Phys. Rev. Lett.* **84**, 3017 (2000).
- [9] K. C. Leptos, J. S. Guasto, J. P. Gollub, A. I. Pesci, and R. E. Goldstein, Dynamics of Enhanced Tracer Diffusion in Suspensions of Swimming Eukaryotic Microorganisms, *Phys. Rev. Lett.* **103**, 198103 (2009).
- [10] E. H. Harris, *The Chlamydomonas Sourcebook*, edited by E. H. Harris, D. B. Stern, and G. B. Witman (Academic Press, New York, 2009).
- [11] B. Eckhardt and S. Zammert, Non-normal tracer diffusion from stirring by swimming microorganisms, *Eur. Phys. J. E* **35**, 96 (2012).
- [12] J.-L. Thiffeault, Distribution of particle displacements due to swimming microorganisms, *Phys. Rev. E* **92**, 023023 (2015).
- [13] R. Jeanneret, D. O. Pushkin, V. Kantsler, and M. Polin, Entrainment dominates the interaction of microalgae with micron-sized objects, *Nat. Commun.* **7**, 12518 (2016).
- [14] A. Brown and W. Poon, Ionic effects in self-propelled Pt-coated Janus swimmers, *Soft Matter* **10**, 4016 (2014).
- [15] S. Michelin and E. Lauga, Geometric tuning of self-propulsion for Janus catalytic particles, *Sci. Rep.* **7**, 42264 (2017).
- [16] Z. Lin, J.-L. Thiffeault, and S. Childress, Stirring by squirmers, *J. Fluid Mech.* **669**, 167 (2011).
- [17] A. Morozov and D. Marenduzzo, Enhanced diffusion of tracer particles in dilute bacterial suspensions, *Soft Matter* **10**, 2748 (2014).
- [18] E. W. Burkholder and J. F. Brady, Tracer diffusion in active suspensions, *Phys. Rev. E* **95**, 052605 (2017).
- [19] V. Sposini, A. V. Chechkin, F. Seno, G. Pagnini, and R. Metzler, Random diffusivity from stochastic equations: Comparison of two models for Brownian yet non-Gaussian diffusion, *New J. Phys.* **20**, 043044 (2018).
- [20] B. Delmotte, E. E. Keaveny, E. Climent, and F. Plouraboué, Simulations of Brownian tracer transport in squirmer suspensions, *IMA J. Appl. Math.* **83**, 680 (2018).
- [21] C. L. Vestergaard, Optimizing experimental parameters for tracking of diffusing particles, *Phys. Rev. E* **94**, 022401 (2016).
- [22] E. H. Harris, *The Chlamydomonas Sourcebook: Introduction to Chlamydomonas and its Laboratory Use* (Academic Press, New York, 2009), Vol. 1.
- [23] B. P. Marsh, N. Chada, R. R. Sanganna Gari, K. P. Sigdel, and G. M. King, The Hessian Blob algorithm: Precise particle detection in atomic force microscopy imagery, *Sci. Rep.* **8**, 978 (2018).
- [24] D. O. Pushkin and J. M. Yeomans, Fluid Mixing by Curved Trajectories of Microswimmers, *Phys. Rev. Lett.* **111**, 188101 (2013).
- [25] M. J. Lighthill, On the squirming motion of nearly spherical deformable bodies through liquids at very small Reynolds numbers, *Commun. Pure Appl. Math.* **5**, 109 (1952).
- [26] X. Michalet, Mean square displacement analysis of single-particle trajectories with localization error: Brownian motion in an isotropic medium, *Phys. Rev. E* **82**, 041914 (2010).
- [27] T. Savin and P. S. Doyle, Static and dynamic errors in particle tracking microrheology, *Biophys. J.* **88**, 623 (2005).
- [28] J. Palacci, C. Cottin-Bizonne, C. Ybert, and L. Bocquet, Sedimentation and Effective Temperature of Active Colloidal Suspensions, *Phys. Rev. Lett.* **105**, 088304 (2010).
- [29] D. Loi, S. Mossa, and L. F. Cugliandolo, Effective temperature of active matter, *Phys. Rev. E* **77**, 051111 (2008).
- [30] M. C. Marchetti, J. F. Joanny, S. Ramaswamy, T. B. Liverpool, J. Prost, M. Rao, and R. Aditi Simha, Hydrodynamics of soft active matter, *Rev. Mod. Phys.* **85**, 1143 (2013).
- [31] A. E. Patteson, A. Gopinath, P. K. Purohit, and P. E. Arratia, Particle diffusion in active fluids is non-monotonic in size, *Soft Matter* **12**, 2365 (2016).
- [32] H. Shimazaki and S. Shinomoto, Kernel bandwidth optimization in spike rate estimation, *J. Comput. Neurosci.* **29**, 171 (2010).
- [33] Note that the superposition of two independent random processes, e.g., thermal noise and random swimmer-induced displacements, results in a convolution of the corresponding pdfs instead of any addition. This assumption is a functional approximation without an underlying model. Our fit parameters for Eq. (1) in Ref. [9] are $f = 0.024$; $A_g = 0.65 \mu\text{ms}^{-1/2}$ and $A_e = 1.82 \mu\text{ms}^{-1/2}$.
- [34] Unlike stated in [11], two parameters are required, the α and the fractional D in units of $\mu\text{m}^{2\alpha}\text{s}^{-\alpha}$. The time cannot be scaled out as claimed. We obtain the parameters $\alpha = 0.975$ and $D = 0.22 \mu\text{m}^{2\alpha}\text{s}^{-\alpha}$.
- [35] See Supplemental Material at <http://link.aps.org/supplemental/10.1103/PhysRevLett.122.148101> for a detailed discussion of a broad velocity distribution.
- [36] D. W. Scott, *Multivariate Density Estimation: Theory, Practice, and Visualization* (John Wiley & Sons, New York, 2015).
- [37] B. Dybiec and E. Gusupldowska-Nowak, Subordinated diffusion and continuous time random walk asymptotics, *Chaos* **20**, 043129 (2010).